Single-crystal NMR spectra of solid H_2 containing very low ortho-H_2 concentrations

J. R. Gaines, A. Mukherjee, and Yan-Chi Shi
Department of Physics, The Ohio State University, Columbus, Ohio 43210
(Received 29 September 1977)

A motional-narrowing model adapted from the work of Anderson is used to interpret anisotropic NMR spectra from samples of solid para-H_2 containing ortho-H_2 impurity concentrations of less than 3×10^{-3}. The experimental data were taken at a Larmor frequency of 30 MHz over a temperature range of 4.2–0.04 K. An analysis of the data at the lowest temperature indicates that the samples are single crystals. Values for the transition probability per unit time between the isolated molecular rotational substates are deduced as a function of temperature for this model. Based on the change of this transition probability with temperature, it is concluded that the samples undergo an order-disorder transition below 0.18 K.

I. INTRODUCTION

The occurrence of a cooperative phase transition in solid H_2 with high ortho-H_2 (o-H_2) concentration (the λ transition) has been studied by various workers using nuclear-magnetic-resonance (NMR),[1] crystallographic,[2] and thermal techniques.[3] Theoretical work[4] showed that the electric quadrupole-quadrupole (EQQ) interaction between the o-H_2 molecules was responsible for driving this phase transition, and that the phase change minimized the EQQ interaction energy. This transition was observed in the o-H_2 concentration range 99 mole % to about 56 mole %, below which it was postulated that EQQ interactions could not bring about a phase transition.

Recent work by Sullivan *et al.*[5] and Ishimoto *et al.*,[6] seems to indicate the occurrence of cooperative ordering in solid H_2 with o-H_2 concentrations below 55 mole %. This conclusion was based on the observation of temperature-dependent structure in the NMR spectra coupled with relaxation-time measurements. From the data of Ishimoto *et al.*,[6] the dependence of the transition temperature T_c on o-H_2 concentration x appears to follow an equation of the form $T_c = 0.15(1+x)$ K in the concentration range $0.075 \lesssim x \lesssim 0.5$. While identification of structure on the NMR line with the occurrence of a phase transition appears reasonable in the light of similar observations at the λ transition, it is important to note that a resolved structure also appears in the nearest-neighbor pair spectrum[7] of dilute ortho-para alloys with no accompanying phase transition.

We present results of systematic pulsed NMR measurements on very dilute ortho-para alloys ($10^{-4} \lesssim x \lesssim 3\times10^{-3}$) in the temperature range 4.2–0.04 K. The free-induction decay (FID) was studied as a function of temperature, the thermal history of the samples, and the orientation of the applied magnetic field. Structure, of an oscillatory nature, was observed to occur on the FID for all the samples in the temperature range 0.11–0.18 K, and the beat frequency was found to be independent of temperature down to the lowest temperatures observed (0.04 K). The pair spectrum characteristic of higher concentrations was not seen. Considerable hysteresis was observed on thermal cycling of the samples, in terms of the temperatures corresponding to the appearance and disappearance of structure, and the beat structure was also seen to be a function of the orientation of the external magnetic field.

These results have been analyzed in terms of a "motional-narrowing" model that incorporates the effect of Markovian motion (to take into account the transitions between the rotational substates of an o-H_2 molecule) on discrete lines in frequency space. In terms of the dimensionless parameter Ω/δ (where Ω is the transition probability per unit time between the rotational substates, and $\delta = \frac{3}{4}d(3\gamma^2-1)$, with d being the intramolecular coupling constant, 57.7 kHz, and γ the cosine of the angle between the magnetic-field direction and the symmetry axis of the crystal), the model predicts structure on the FID when $|\Omega/\delta|<1$ and no structure (pure exponential decay) when $|\Omega/\delta|>1$. The actual structure observed, together with the associated damping, conforms favorably to the predictions of the model, and gives values for Ω as a function of temperature and the magnitude and sign of the splitting between the rotational levels. Experimental values for the change in Ω with temperature indicate an abrupt change in Ω (by a factor of more than 10) over a narrow temperature interval for all the samples studied. This, together with the hysteresis observed, leads to the conclusion that a cooperative phase transition is occurring even at these very low concentrations. The transition temperatures corresponding to the onset of structure agree with an extrapolation of Ishimoto's higher-concentration data down to $x=0$.

Finally, the dependence of the structure observed on the orientation of the external magnetic field is used, on the basis of the above model, to establish the single-crystal nature of the samples, with a substantial projection of the symmetry axis (c axis) on the plane of rotation of the magnet. A method is also proposed, by which the crystalline state of a sample of solid H_2 may be obtained using only high-temperature (~4.2-K) NMR measurements.

II. THEORY

Because of the large distances between near neighbors at such low concentrations, the individual o-H_2 molecules constitute a noninteracting magnetic ensemble with secular Hamiltonian in the interaction representation

$$H' = -c\gamma J_\xi I_z + \tfrac{1}{4}d(3\gamma^2 - 1)(3J_\xi^2 - 2)(3I_z^2 - 2) \qquad (1)$$

(in angular frequency units), where c is the spin-rotation interaction coupling constant, d is the intramolecular dipolar coupling constant, I_z is the projection of the total spin ($I = 1$) on the magnetic field direction, J_ξ is the projection of the rotational angular momentum ($J = 1$) on the crystal c axis, and γ is the cosine of the angle between the c axis and the magnetic field.

For NMR absorption where $\Delta m_I = -1$, discrete lines are obtained at $\omega_0 + c\gamma J_\xi \pm \delta(3J_\xi^2 - 2)$ where $\delta = \frac{3}{4}d(3\gamma^2 - 1)$ and ω_0 is the Larmor frequency. Thus, the rotational substate expectation value is critical to the position of the line in frequency space. Two cases will be treated: (a) If we characterize J_ξ by the values +1, 0, and −1, the spectrum has discrete lines at $\omega_0 + \delta \mp c\gamma$ and $\omega_0 - 2\delta$, and similar lines with δ replaced by $-\delta$. (b) If instead of the above states of J_ξ one chooses the states

$$|s\rangle = (1/\sqrt{2})(|1\rangle + |-1\rangle),$$
$$|a\rangle = (1/\sqrt{2})(|1\rangle - |-1\rangle) \quad \text{and} \quad |0\rangle,$$

then the spectrum has discrete lines at $\omega_0 - 2\delta$ (as before) and $\omega_0 + \delta$ (twice). This choice of states "quenches" the rotational angular momentum.

In both cases, however, the spectrum contains a finite number (three) of discrete (infinitely sharp) lines if J_ξ remains constant during the time period necessary to observe the NMR signal. If, however, transitions occur between the states characterizing the rotational subsystem, one has a situation analogous to the famous "motional-narrowing problem" or "exchange-narrowing problem." In this case, rapid transitions can coalesce the resolved resonance lines into a single line centered at ω_0. In 1954, Anderson[8] presented a model of this type of process that can be easily adapted to this specific problem.

The signal following a radio frequency (rf) pulse that produces a rotation θ_1 of the magnetization from the equilibrium direction can be written

$$S(t) = \mathrm{Tr}[\rho'(t) I_+]/\mathrm{Tr}[\rho'(0) I_+], \qquad (2)$$

where

$$\rho'(t) = \exp\left(-i\int_0^t H'(t')\,dt'\right)\rho'(0) \times \exp\left(i\int_0^t H'(t')\,dt'\right),$$

$$\rho'(0) = \exp(i\theta_1 I_y)\rho(0)\exp(-i\theta_1 I_y),$$

and

$$\rho(0) = \exp[-(\hbar\omega_0 I_z/k_B T)] \cong 1 - (\hbar\omega_0/k_B T) I_z,$$

in the "high-temperature" approximation. After some straightforward algebra we obtain

$$S(t) = \sin\theta_1 \left\langle \exp i\int_0^t \omega'(t')\,dt' \right\rangle, \qquad (3)$$

where

$$\omega'(t') = -c\gamma J_\xi(t') + \delta[3J_\xi^2(t') - 2].$$

Following the elegant presentation of the motional-narrowing problem found in Abragam's treatise,[9] one evaluates $S(t)$ under the assumption that the hopping from one frequency to another in the spectrum of discrete lines is a stationary Markov process. The probability that the frequency ω has the value ω_2 at time $t' = t + \Delta t$ when it is known to have had value ω_1 at time t is denoted by $W(\omega_1 | \omega_2 \Delta t)$. For short time intervals Δt, W can be expressed as

$$W(\omega_1 | \omega_2 \Delta t) = \delta_{\omega_1,\omega_2} + \pi(\omega_1, \omega_2)\Delta t. \qquad (4)$$

Defining $\Omega(\omega_1)$ as the transition probability per unit time that the system will pass from a frequency ω_1 to a *different value*, we can note

$$\Omega(\omega_1) = -\pi(\omega_1, \omega_1), \qquad (5a)$$

$$\sum_{\omega_2} \pi(\omega_1, \omega_2) = 0, \qquad (5b)$$

since $\sum_{\omega_2} W(\omega_1 | \omega_2 \Delta t) = 1$.

For the moment, ignore the factor $\sin\theta_1$ and note that the FID can be written in the form $S(t) = \sum_{\omega_\alpha} S_\alpha(t)$ where the ω_α are the discrete frequencies in the spectrum. After some manipulation this yields

$$S(t) = \vec{S} \cdot \exp[(i\underline{\omega} + \underline{\pi})t] \cdot \vec{1}, \qquad (6)$$

where $\vec{S}$ is a vector with components $S_\alpha(0)$, $\vec{1}$ is a vector with all components equal to unity, $\underline{\omega}$ is a matrix with components $(\underline{\omega})_{\alpha\beta} = \omega_\alpha \delta_{\alpha\beta}$ and $\underline{\pi}$ is the

matrix with components $(\underline{\pi})_{\alpha\beta} = \pi(\omega_\alpha, \omega_\beta)$.

It is possible at this point to calculate the absorption $I(\omega)$ by computing the Fourier transform of the above expression or one can use the techniques of matrix algebra to compute $S(t)$ directly. The latter approach will be followed as it is more appropriate to the experimental results described in this paper. The key to this approach is to find the eigenvalues λ_i of the operator

$$\underline{M} = i\underline{\omega} + \underline{\pi}, \tag{7}$$

and to construct the matrices T and T^{-1} (from the orthonormal eigenvectors of $\underline{M}$) that diagonalize $\underline{M}$ giving $\underline{TMT^{-1}} = \underline{\Lambda}$. If we denote the three eigenvalues by λ_u, λ_v, and λ_w and assign corresponding eigenvectors the components u_1, u_2, u_3, etc., then the general result for this three level system is[10]

$$S(t) = e^{\lambda_u t}(u_1+u_2+u_3)^2 + e^{\lambda_v t}(v_1+v_2+v_3)^2 + e^{\lambda_w t}(w_1+w_2+w_3)^2 . \tag{8}$$

We evaluate this expression for the two cases considered earlier. For case (a) the most general form for the matrix π consistent with the sum rules 5(b) and detailed balancing leads to the following form for $\underline{M}$:

$$\underline{M} = \begin{bmatrix} i(\delta - c\gamma) - (\Omega/q) & \Omega & [(1-q)/q]\Omega \\ \Omega & i(-2\delta) - 2\Omega & \Omega \\ [(1-q)/q]\Omega & \Omega & i(\delta + c\gamma) - (\Omega/q) \end{bmatrix}, \tag{9}$$

where q is the relative probability of going to state $|0\rangle$ from state $|1\rangle$ and $\Omega(0) = 2\Omega$. The above form for $\underline{M}$ leads to a cubic equation for λ that can be solved numerically for specific choices of parameters. Considerable insight can be gained by applying perturbation theory to this problem.

By neglecting the off-diagonal elements in $\underline{M}$ we can obtain an expression for the FID that should be valid to a first approximation when the transitions are not rapid enough to wash out the discrete lines

$$S_s(t) \cong 2\cos(c\gamma t)e^{i\delta t}e^{-\Omega t/q} + e^{-2i\delta t}e^{-2\Omega t}. \tag{10}$$

To find the FID in the limit of fast transitions, one can find the eigenvalues and eigenfunctions of the matrix π and then obtain the lowest-order corrections arising from ω. The first-order correction vanishes so that in second order

$$S_F(t) \cong 3\exp\left[-\left(\frac{2c^2\gamma^2}{3\Omega[(2/q)-1]} + \frac{2\delta^2}{3\Omega}\right)t\right]. \tag{11}$$

The matrices π and ω are simplified by the second choice of states $|s\rangle$, $|a\rangle$, and $|0\rangle$ as the term involving the spin-rotation interaction in ω drops out. Since both $|s\rangle$ and $|a\rangle$ give rise to the same discrete frequency, transitions between these states are unobservable (the result is the same as taking $q = 1$). We now interpret Ω as the transition probability per unit time out of $|s\rangle$ or $|a\rangle$ (and into $|0\rangle$). Thus, $\underline{M}$ becomes

$$\underline{M} = \begin{bmatrix} i\delta - \Omega & \Omega & 0 \\ \Omega & -2i\delta - 2\Omega & \Omega \\ 0 & \Omega & i\delta - \Omega \end{bmatrix}, \tag{12}$$

which gives the following equation for the eigenvalues λ:

$$(i\delta - \Omega - \lambda)[(i\delta - \Omega - \lambda)(2i\delta + 2\Omega + \lambda) + 2\Omega^2] = 0. \tag{13}$$

If we define the dimensionless ratio $x = \delta/\Omega$, then we write the eigenvalues as $\lambda_1 = ix - 1$, $\lambda_2 = -\frac{1}{2}(3+ix) + \frac{3}{2}(1 - x^2 + \frac{2}{3}ix)^{1/2}$, and $\lambda_3 = -\frac{1}{2}(3+ix) - \frac{3}{2}(1 - x^2 + \frac{2}{3}ix)^{1/2}$. Computing the eigenvalues and substituting into the general expression (8) gives the very simple result

$$S(t) = [3/(\lambda_3 - \lambda_2)](\lambda_3 e^{\lambda_2 t} - \lambda_2 e^{\lambda_3 t}). \tag{14}$$

In this form, one can easily approximate the values of λ_2 and λ_3 in the two extreme limits of slow ($x > 1$) and rapid ($x < 1$) transition. For slow transitions, to lowest order,

$$S_s(t) \cong 2e^{i\delta t}e^{-\Omega t} + e^{-2i\delta t}e^{-2\Omega t}, \tag{15}$$

whereas for the rapid transitions, correct to second order, one finds

$$S_F(t) \cong 3\exp[-(2\delta^2/3\Omega)t]. \tag{16}$$

The simple perturbation theory used earlier gives precisely these results when $\underline{M}$ from Eq. (12) is used. Higher-order corrections can be easily included but for most cases, numerical solutions would be more desirable.

The expressions for the FID that will be compared to the experimental results all contain γ, the cosine of the angle between the magnetic-field direction and the crystalline c axis so that knowledge of the quantity is important for a detailed comparison. If the samples are polycrystalline then an average over γ must be taken which yields a Pake doublet line shape that has been previously

obtained by Reif and Purcell[11] when $\Omega = 0$. In the limit of rapid transitions, it is appropriate to replace γ'' in the expression for $S(t)$ by the spherical average value for a powder, for short times $t < T_2$.

The overall features of the pairs of equations (10) and (15) and (11) and (16) are the same. The latter two both have the motionally narrowed form in the fast transition limit whereas the former are damped oscillatory FID's in the slow transition limit with different damping factors on the two terms. The one outstanding difference is the prediction [Eq. (11)] that a modulation due to the spin-rotation interaction will be seen on the signal with frequency δ *but not on the one with frequency* 2δ. It can be seen that the argument that rapid transitions between the states $m_J = \pm 1$ would wash out this structure indicates that q would be a very small number so that the frequency δ would be much more heavily damped than the frequency 2δ (i.e., the frequency δ would have to be critically damped or overdamped).

Thus, if the signal at frequency δ is observed, a measure of its damping rate and the existence of any modulation would be the test of the state classification scheme. In a previous experiment, Constable and Gaines[12] observed the signal in the slow transition limit. They observed *no modulation characteristic of the spin-rotation interaction*; two signals at frequencies $\frac{3}{4}d$ and $\frac{3}{2}d$, and damping factors that differed by about a factor of 2 with the high-frequency component being the most heavily damped. As our present experimental results are entirely consistent with the previous ones, *we conclude that the most reasonable set of states is the set* $|s\rangle$, $|a\rangle$, *and* $|0\rangle$.

There are two important factors that can influence the line shape of the observed signal that have not been discussed previously: (i) Boltzmann weighting of the relative components and (ii) a pulse-width correction arising from the fact that not all the spins in the frequency spectrum receive the same rf power and hence the same rotation θ_1. The latter correction is only important in the slow transition limit. The rotation angle is computed from the pulse power spectrum and the frequency-dependent correction term is incorporated in the final expression for $S(t)$. The first correction can be incorporated by multiplying each of the vector components S_α of the vector $\vec{S}$ by the appropriate Boltzmann factors. It is through this correction that one can estimate the splitting between the m_J sublevels for a given temperature. For instance, if we assume that the states $|s\rangle$ and $|a\rangle$ are degenerate and separated in energy from the state $|0\rangle$ by A units of energy due to a crystal field interaction, then

$$H_{CF} = \tfrac{1}{3}A(3J_\zeta^2 - 2), \tag{17}$$

and Eq. (15) becomes

$$S_s(t) = \frac{2e^{i\delta t}e^{-\Omega t}e^{-A/k_BT}f(\delta) + e^{-2i\delta t}e^{-2\Omega t}f(2\delta)}{2e^{-A/k_BT}+1}, \tag{18}$$

where

$$f(x) = \sin[\tfrac{1}{2}\pi \sin(\tfrac{1}{2}xt_p)/(\tfrac{1}{2}xt_p)],$$

with t_p the time duration of the rf pulse.

A resolvable splitting on the NMR absorption line will correspond to the appearance of sines and cosines (imaginary exponentials) in the FID. Because the condition that differentiates between the "slow" and "fast" transition limits involves the angular factor γ one can have the interesting possibility in the "slow transition limit" that while $\frac{3}{4}d > \Omega$ that $\delta < \Omega$ if $3\gamma^2 - 1 \approx 0$. It is the location of this "magic angle" that permits us to determine the orientation of the c axis of our crystal by NMR techniques.[13]

For a given orientation of the magnet (fixed γ) a change in the NMR line from one with no structure (damping only) to one with structure (damping plus oscillatory terms) is due to a change in Ω. The application of the results of this model makes it possible to obtain numerical values for Ω in both limits discussed here. In the fast transition limit, the FID is predicted to be a simple exponential $[\exp(-t/T_2')]$ where $T_2' = 3\Omega/2\delta^2$. Universal behavior is expected then at sufficiently low concentrations for this model to be valid with Ω acting as the scaling parameter. In the slow transition limit, Ω is measured directly from the damping of the oscillatory terms at frequencies δ and 2δ.

Furthermore, changes in Ω as a function of temperature can be used to study phase transitions in this system.[14] By knowing the crystalline state of the system, Ω can be obtained from the FID at all temperatures in principle. Since Ω is the transition probability per unit from $|a\rangle$ or $|s\rangle$ to $|0\rangle$, we can use the changes in Ω and hence the NMR spectrum to probe the interactions between the rotational sublevels and the phonons.

III. EXPERIMENTAL PROCEDURE

The hydrogen samples were cooled in a dilution refrigerator capable of maintaining a temperature of about 15 mK under "no load" conditions. The cooling characteristics of the refrigerator have been discussed in detail elsewhere,[15] but it is relevant to note here that the lowest temperature reached should depend on the concentration of o-H_2 present in the sample as the conversion from o-H_2 to p-H_2 generates heat in the solid. Although this variation was observed over a concentration range of $x = 3 \times 10^{-3}$ to $x = 10^{-1}$,[16] no appreciable change in

the lowest temperature obtained was noted in the concentration range 10^{-4} to 3×10^{-3}. Thus, 40 mK appears to be the lowest temperature to which we can cool a hydrogen sample in our refrigerator.

A. Sample preparation

All the samples are prepared in a separate apparatus. Normal hydrogen from a cylinder was passed through a cold trap (N_2) and into the sample cell of a Cryotip refrigerator. A chrome alumina catalyst was used to convert the liquid H_2. The liquid vapor pressure was maintained between 250 and 625 Torr for periods of 3–10 h depending on the o-H_2 concentration desired. During this time, the sample bulbs were flushed with hydrogen and evacuated at regular intervals. The o-H_2 concentrations obtained were in reasonable agreement with the Boltzmann equilibrium concentrations at the temperatures corresponding to the measured vapor pressures. The process of transferring the sample bulb to the dilution refrigerator filling the sample cell, and cooling the sample to 4.2 K typically took about an hour. The sample cell was made of glass and oxygen-free high-conductivity copper, and has been discussed in detail elsewhere,[15] but it is relevant to note here that thermal contact between the sample and the mixing chamber was achieved by the column of hydrogen itself extending into the copper cylinder which acts as the heat exchanger. The NMR coil surrounded only the glass portion of the cell. As the sample cell was being filled, the amount of exchange gas in the vacuum jacket was controlled to keep the temperature just around the melting point, with liquid helium only in the tail of the Dewar. Thus, the sample cell was in a region of uniform temperature. Once the cell was full, the sample temperature was instantly cooled to 4.2 K.

B. Determination of the concentration

After cooling the sample to 4.2 K, a free-induction decay signal was recorded. The initial height of this signal gave the magnetization at time $t=0$ and the decay rate gave T_2, the transverse relaxation time. The concentrations were determined using the Hardy and Gaines[17] measurements of T_2 as a function of concentration. This method was satisfactory for $x=3\times10^{-3}$ and $x=2\times10^{-3}$ but for the lowest concentration no such comparison was possible. Thus the signal heights at 1 K were compared to estimate the concentration value of $x\simeq10^{-4}$. The upper limit on this concentration was 5×10^{-4}.

C. Electronics

The pulsed NMR system had four basic components: (i) the transmitter, (ii) the probe, (iii) the receiver, and (iv) the analyzer. A 30-MHz crystal controlled oscillator was used to provide a high-power rf pulse. A 90° pulse was obtained in 8 μsec. The output of the reference oscillator was split into two channels. The first went through an attenuator to the receiver and served as the reference signal for the phase-sensitive detector; the second channel fed directly into an rf gate. The output of the gate was fed into the transmitter. The response of the phase-sensitive detector was checked to be linear. Its output was monitored on an oscilloscope and fed to the signal-averaging system. This system consisted of a Biomation (Model 802) transient recorder coupled to a Nicolet (Model 1070) signal averager. The Nicolet was interfaced with a Kennedy (Model 9700) tape recorder that facilitated data storage and retrieval. The dead time in the receiver was about 3 μsec.

D. Thermometry

Several different thermometers were used to cover the temperature range from room temperature down to 0.04 K. From room temperature down to 4.2 K, a silicon diode (D689) was used. In the range 4.2–0.1 K, two germanium thermometers with overlapping ranges were used. The thermometers have been calibrated previously against cerous magnesium nitrate and platinum NMR measurements. Estimated errors in the temperature determinations were ±1% from 4.2 to 0.1 K and ±5% in the range 0.1–0.04 K.

E. Experiments

Three different concentrations were studied, $x=3\times10^{-3}$, $x=2\times10^{-3}$, and $x\simeq10^{-4}$. Reproducible and repeatable results obtained for each of the above concentrations on more than one run.

The free-induction decays were studied systematically as a function of temperature for all the samples. In particular, the temperature at which oscillatory structure first appeared on cooling the various samples was carefully noted as well as the temperatures for which the structure almost disappeared on warming up. Care was taken to ensure that the sample was in thermal equilibrium with the mixing chamber of the dilution refrigerator after each sequence of pulses. This was checked for the $x\cong10^{-4}$ sample down to 0.1 K using the "internal thermometer" provided by the nuclear spins. This is described in more detail later. The temperature dependence of the frequency of the oscillatory structure was also studied as was the magnetic-field orientation-dependence of the structure.

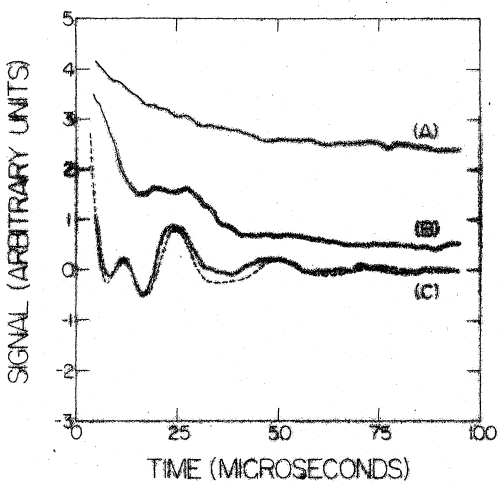

FIG. 1. Free-induction decays for the $x = 10^{-4}$ samples: (a) at $T = 0.20$ K (before structure appeared); (b) at $T = 0.13$ K (just after structure appeared); (c) at $T = 0.04$ K. The dashed line is the theoretical line shape obtained after correcting for the effects of pulse-width variation and the baseline for $\Omega = 4.5 \times 10^4$ rad/sec, $A = +0.044$ K, and $\delta = -\frac{3}{4}d$. The solid line is the experimental free-induction decay. The vertical scale applies only to trace C.

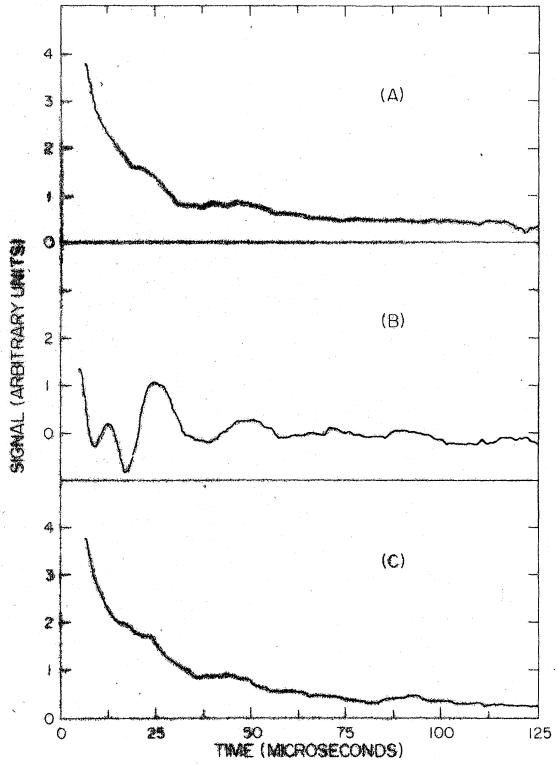

FIG. 2. Free-induction decay as a function of magnetic field orientation (ϕ) for the $x \simeq 10^{-4}$ sample at 0.04 K. (a) $\phi \simeq 15°$ (with respect to an arbitrary zero); $\delta = 0$. (b) $\phi \simeq 60°$; $\delta = \frac{3}{4}d$. (c) $\phi \simeq 105°$; $\delta = 0$.

IV. RESULTS AND ANALYSIS

In Fig. 1 (traces A and B), the typical onset of structure when the sample is cooled down is shown. The gross features of the transition from "no structure" to "structure" while cooling are the same for all magnet orientations except at the "magic angle" value where $3\gamma^2 - 1 = 0$. The beats once noticed are characterized by a frequency that is essentially independent of temperature. However, the damping does change with temperature near the transition temperature. The analogy of this system with a damped harmonic oscillator passing from the overdamped through the critical case and into the underdamped behavior is a good one (but not perfect due to the two frequencies present in the underdamped state). Upon increasing the temperature a pronounced hysteresis is observed and the structure does not completely disappear even at 0.6 K.

In Fig. 2, the angular dependence of the FID is shown at the lowest temperature reached in this experiment (0.04 K). It is seen that in traces A and C the oscillatory FID, which is seen in trace B, is absent. Thus, even for $T < T_c$, if $\delta = 0$ as in A and C no structure is seen now as predicted by the motional narrowing model. The FID in trace B corresponds to $|\delta| = \frac{3}{4}d$. Two cones of semiangle 54.7° drawn about the magnet orientation when $\delta = 0$ intersect above (and below) the plane in which we rotate the magnet. The projection of the c axis on this plane lies intermediate between the two magic angle positions and makes an angle of 35.2° with respect to the c axis. Thus, at this position $3\gamma^2 - 1 = 1$ and $\delta = \frac{3}{4}d$ is observed. These results were not reproducible between crystallizations.

This result, by itself, is strong confirmation that the motional-narrowing model is a valid one to apply to this system. In addition, one must apply the predictions of this model to the *single-crystal case* to obtain a result such as that shown in Fig. 2 as the quenching of the oscillatory component would not be complete if there were several oriented crystallites.

Knowledge of the crystalline state of the sample makes it possible to computer fit the slow transition result, Eq. (18), to the observed FID with a reduced number of adjustable parameters. It is assumed that δ is known in addition to the temperature so the only adjustable parameters are Ω and A (sign and magnitude). Shown in Fig. 1 (trace C) is a computer fit that best resembles our observed FID. Although the fit is not perfect, it reproduces satisfactorily most of the notable features. It should be noted that the sign of A chosen here is

opposite to that of Constable and Gaines[12] and makes the nondegenerate state $m_J = 0$ the ground state. In their experiment, angular dependence was not tested for, and the powder average line shape was used to obtain the mix of the two signals at $\frac{3}{4}d$ and $\frac{3}{2}d$ before Boltzmann weighting (containing the parameter A) was introduced.

We have computed the powder average line shape that is predicted by the motional-narrowing model. For arbitrary ratio Ω/δ the absorption intensity is given by

$$I(\omega) = \frac{3\omega\Omega\delta(3p_0 - 1) - 6\Omega\delta^2}{(2\delta + \omega)^2(\delta - \omega)^2 + (3\omega\Omega)^2} - \frac{3\omega\Omega\delta(3p_0 - 1) + 6\Omega\delta^2}{(\omega - 2\delta)^2(\omega + \delta)^2 + (3\omega\Omega)^2}. \quad (19)$$

For the case $\Omega = 0$, the integral (weighting all increments of solid angle equally) gives a superposition of the two Pake doublets (with Boltzmann factors) previously given by Reif and Purcell.[11] For $\Omega \neq 0$, the powder average can differ markedly from the superposition of two Pake doublets.

The powder averaged line shape used by Constable and Gaines was correct for $\Omega = 0$ (although it was only assumed that the samples were not single crystals) but for $\Omega/d \cong 0.2$ (as they observed) it would be incorrect and seriously affect the magnitude and sign of the crystal-field splitting determined by a fit of the data to the theoretical line shape.

To illustrate this point we compare the ratio of the signal at $t = 25$ μsec to that at $t = 12.5$ μsec using the expressions given by Constable and Gaines to that predicted by our present single-crystal analysis, Eq. (18). By equating these two expressions, which can be evaluated numerically, we obtain a relationship between the population factor used by Constable and Gaines (which we designate p_1) and the population factor necessary to obtain *the same ratio* from the present work (which we designate p_2):

$$p_1 = \exp(-A_1/k_B T) \quad \text{and} \quad p_2 = \exp(-A_2/k_B T). \quad (20)$$

In the notation of Constable and Gaines

$$\frac{S(t_2)}{S(t_1)} = \frac{G_0(t_2)e^{-\delta_0 t_2} + 2p_1 G_1(t_2)e^{-\delta_1 t_2}}{G_0(t_1)e^{-\delta_0 t_1} + 2p_1 G_1(t_1)e^{-\delta_1 t_1}}. \quad (21)$$

The same ratio based on the present work is

$$\frac{S_s(t_2)}{S_s(t_1)} = \frac{2e^{i\delta t_2}e^{-\Omega t_2}p_2 f(x) + e^{-2i\delta t_2}e^{-2\Omega t_2}f(2x)}{2e^{i\delta t_1}e^{-\Omega t_1}p_2 f(x) + e^{-2i\delta t_1}e^{-2\Omega t_1}f(2x)}. \quad (22)$$

Equating these two results for the ratio and evaluating numerically we obtain

$$p_2 = [(0.3276)p_1 + 0.0710]/(p_1 + 0.8600). \quad (23)$$

If we now substitute $T = 40$ mK and $A_1 = -23$ mK as found by Constable and Gaines, we obtain $A_2 = +56$ mK. Using the same input, namely, the ratio of two suitably chosen signal heights, the present analysis would give both a different magnitude and sign for A from that assigned by Constable and Gaines. Thus, knowledge of the crystalline state of the sample is critical to the determination of the crystal-field splitting.

Due to poor signal-to-noise ratio and the effect of the pulse-width correction on the results, we were unable to observe the temperature dependence of the relative intensities of the two signals (at δ and 2δ). From such an observation, one should be able to make an unambiguous determination of the size (and sign) of the crystal-field interaction. The result quoted here for A can be considered to be reliable only to within a factor of two.

One very interesting plot that can be generated from these data is a graph of the variation in the parameter Ω with respect to temperature. In the fast transition limit (no structure on the line) the FID is essentially of the form $S(t) \sim e^{-t/T_2}$ so that by measuring the experimental T_2, using the result $(1/T_2) = \frac{2}{3}\delta^2/\Omega$, and the value of δ from the angular-dependence study, the value of Ω is obtained. In the slow transition limit, Ω is obtained directly from the damping of the FID as predicted in Eq. (18). Obtained in this manner, the values of Ω are extremely model dependent and thus valid to the extent that the model gives an accurate description of this real physical system. The values of Ω deduced as described above are shown in Fig. 3 where the dimensionless parameter Ω/d is given as a function of temperature. It should be noted that Ω is essentially independent of temperature except in the immediate vicinity of the transition temperature T_c.

The change in the observable NMR properties, namely, the line shape, is by this method related to the change in one parameter Ω, the transition probability per unit time between the molecular sublevels due to interaction with the lattice (phonons). A measurement of Ω thus gives information about the coupling between the rotational degrees of freedom and the phonons in this low-concentration regime and the change in Ω by an order of magnitude at T_c may provide a more accurate picture of crystalline-field effects.

Another indication that a phase transition has occured at T_c is the pronounced hysteresis upon thermal cycling seen in Fig. 3. The structure on the FID that appears quickly upon reducing the temperature below 0.18 K disappears very slowly upon warming and is not completely gone at 0.6 K. It is the combination of the relatively sharp change in Ω upon cooling and the associated hysteresis

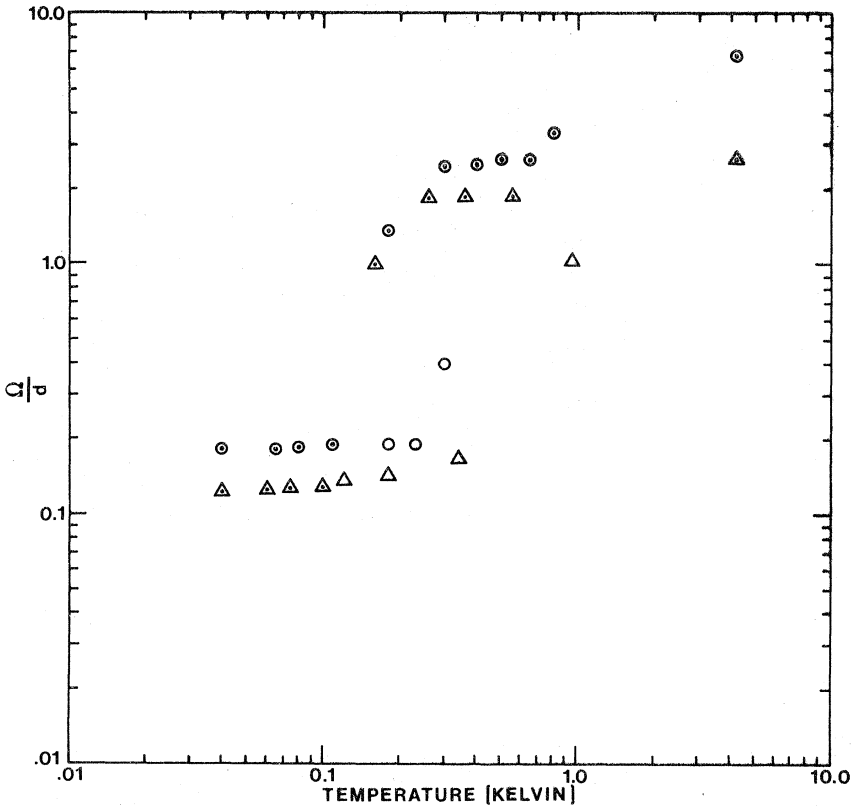

FIG. 3. Variation of Ω/d with temperature. ⊙ represents points obtained for the $x = 3 \times 10^{-3}$ sample while cooling down. ($x = 2 \times 10^{-3}$ gave overlapping points, hence is not shown in the figure). ○ represents points for the $x = 3 \times 10^{-3}$ sample while warming up. △ represents points for the $x \cong 10^{-4}$ sample while cooling down. △ represents points for the $x \cong 10^{-4}$ sample on warming up.

that leads us to call this an order-disorder transition. A comment is in order here regarding the determination of the sample temperature, and establishing that the sample was in equilibrium with the mixing chamber. The free-induction decays observed had a rapidly decaying (fast relaxing) initial slope and a much more slowly relaxing "tail." This slow relaxing part was interpreted earlier[12] as due to remnant HD in the sample. However that may be, the initial height of this signal scaled with temperature according to Curie's law down to 0.1 K. Below 0.1 K, the appearance of pronounced structure on the line made a determination of Curie law scaling very difficult. At the lowest temperatures (~0.04 K), the mixing-chamber thermometers indicated sample heating on application of the pulses and the thermometers relaxed back to 0.04 K after the pulses were stopped. This indicated that the sample was indeed at 0.04 K. Although the spectra in Figs. 1 and 2 are the signal averaged FID's from a number of successive pulses, the time interval between the pulses was such as to allow the sample to relax back to its initial temperature (as indicated by the mixing-chamber thermometers). We have suggested earlier that a long-range interaction of the Suhl-Nakamura type may be responsible for this transition but there are surely other possibilities that must be investigated. Clearly it would be of great interest to have specific-heat measurements to compare with the NMR results but they will be very difficult measurements to make.

As mentioned previously, a correction has been applied to the computer fits based on Eq. (18) that is dependent upon the rf pulse width. This correction is shown in Fig. 4 for the various values of the pulse width. A better design could eliminate this correction altogether but unless it is applied to our data, the observed FID's do not agree with the computer fits near the origin ($t = 0$). It is this region that is of particular interest as it is only near $t = 0$ that one can observe the "$\frac{3}{2}d$" signal due to its larger damping. It should be noted that as the pulse width increases, for fixed transmitter voltage, that the relative heights of the "$\frac{3}{2}d$" and "$\frac{3}{4}d$" signals change in such a way that the "$\frac{3}{4}d$" signal appears more prominent for longer pulse lengths. Specifically, if there is insufficient power to produce a 90° pulse, the uncorrected FID would favor the signal from $m_J = \pm 1$ and could lead to an incorrect value for the crystal field splitting—*both in magnitude and sign*. The experimental results we obtain for various pulse widths are in good agreement with the calculations shown in Fig. 4

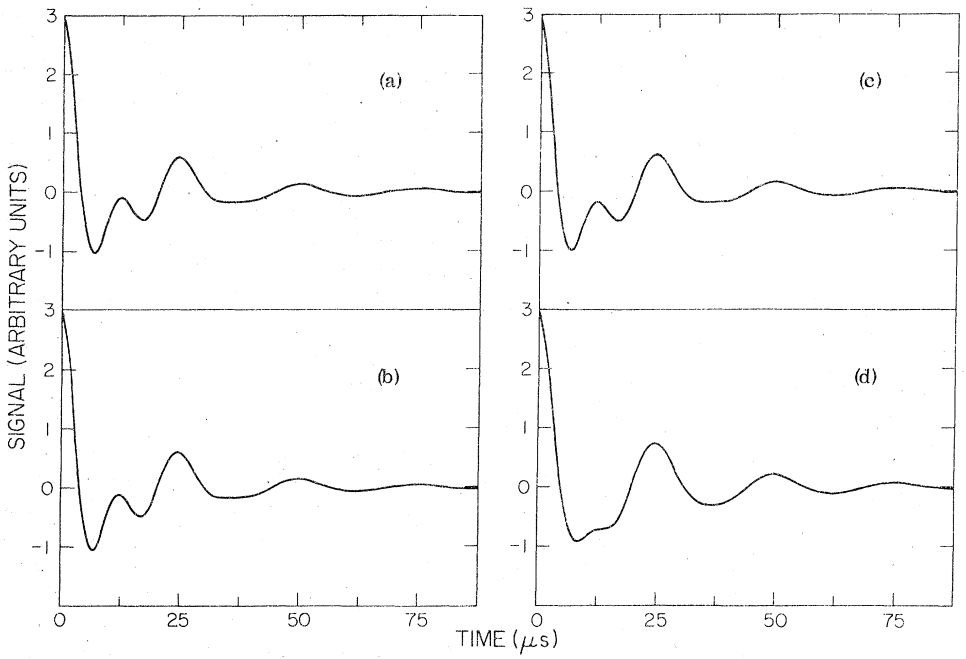

FIG. 4. Pulse-width correction. Theoretical line shapes computed from Eq. (18), for $\Omega = 45 \times 10^4$ rad/sec, $A = 44$ mK, $T = 40$ mK, and pulse widths of (a) 2 μsec, (b) 4 μsec, (c) 6 μsec, and (d) 10 μsec.

but at present as we reduce the pulse width (increasing the width of the power spectrum), we also lose signal since we do not have enough power to produce a 90° pulse for all the spins. The pulse-width correction along with the very poor intrinsic signal-to-noise ratio complicates the determination of A considerably.

In Fig. 5 we give some experimental curves for the FID in the fast transition limit along with a calculated powder average of Eq. (16). For the model we have used, there are no pairwise interactions incorporated so no explicit concentration dependence is predicted. Rather, T_2 is seen to depend only on angle and Ω. Experimentally it is known that T_2 is a function of concentration, decreasing with decreasing o-H_2 concentration. For known angle (or for a powder), the FID predicted in the fast transition limit is a universal curve where Ω acts as a scaling parameter. For practical reasons, if a powder is the appropriate crystalline state, the initial slope of the logarithm of the experimental FID can be used as the scaling parameter as it is simply related to Ω and the spherical average value of $(3\gamma^2 - 1)^2$ (which is equal to $\frac{4}{5}$):

$$\lim_{t \to 0} \frac{d}{dt} \ln S_F(t) = -\frac{1}{T_{2i}} = -\tfrac{2}{3}(\tfrac{3}{4}d)^2 \frac{1}{\Omega} \langle (3\gamma^2 - 1)^2 \rangle_\gamma . \quad (24)$$

Thus, even if the sample is polycrystalline, $\Omega(x)$ can be determined from the initial slope.

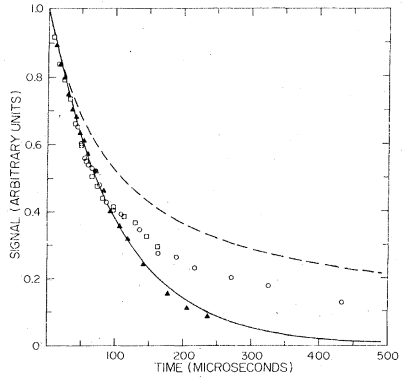

FIG. 5. Comparison of theoretical powder averaged line shape (dashed line) with normalized experimental points ○: $x \simeq 1 \times 10^{-4}$, $T = 0.6$ K, □: $x \simeq 3 \times 10^{-3}$, $T = 0.6$ K. ▲: $x \simeq 1 \times 10^{-2}$, $T = 4.2$ K. The solid line represents pure exponential decay.

V. CONCLUSIONS

In this paper we have presented details of a model that incorporates the ideas of motional narrowing of spectral lines. The model applied to the extremely simple physical situation presented by a low concentration of o-H_2 molecules in solid para-H_2, makes predictions about the NMR line shape in terms of only one parameter, namely the ratio Ω/δ. The excellent qualitative agreement between the model predictions and the observed

NMR spectra leads one to some interesting quantitative predictions. (i) The samples must be single crystals with a substantial projection of the c axis on the plane of rotation of the magnet to agree with the angular dependence predicted by the model. (ii) The transition probability per unit time Ω must be a function of temperature as shown in Fig. 3. The marked decrease in Ω at T_c combined with the observed hysteresis is evidence that a phase transition has occurred. (iii) The FID in the fast transition limit is a universal curve for all concentrations (for which the model applies) with Ω acting as the scaling parameter. A different form of universal curve is obtained for a powdered sample.

Even at higher concentrations where our specific model is inapplicable , the basic approach outlined here that is based on the motional-narrowing concept should yield fruitful results. It should be obvious that in more complicated physical situations it will not be possible to obtain results dependent only on one parameter. Furthermore, from our model, it is clear that unless the transitions between the rotational substates can be neglected entirely ($\Omega = 0$) the line shapes in solid H_2 will be strongly affected.

One interesting speculation is that the powder average of a line shape computed (using the motional-narrowing approach) for much higher concentrations might explain the "incomplete transition" observed there. A transition is said to be incomplete if there is still an appreciable intensity at the center long after ordering has produced splitting of the rest of the line. It has been tentatively assumed that this central line came from regions of the sample with lower o-H_2 concentrations than the average. Such an explanation is based on the expectation that the line shape will be a superposition of Pake doublets below T_c unless there is a concentration inhomogeneity. We would approach this result by noting that if transitions between the sublevels are not completely negligible, then the powder average line shape contains a central peak coming from crystallites where $3\gamma^2 - 1 \cong 0$ and that even at temperatures well below T_c such a central line would still be observable (depending on Ω) and the transition would appear to be incomplete. Line shapes of the type we are describing are observed (i) for $0.15 < x < 0.55$ where a phase transition occurs and (ii) for $0.55 < x$ where a phase transition (the λ transition) driven by nearest-neighbor EQQ interactions occurs.

The experimental results obtained here at the lowest temperatures reached were in good agreement with the earlier results of Constable and Gaines. The analysis presented here is more complete in that the observed angular dependence in these experiments enabled us to determine the crystalline state of our sample. The values of the damping parameters used by Constable and Gaines are in good agreement with ours (although their units should be rad/sec not $\sec^{-1}$) but the sign and magnitude of A is different. These differences are attributed to a combination of poor signal-to-noise ratio (in *both* experiments), inadequate rf power, and usage of an incorrect theoretical line shape by Constable and Gaines.

ACKNOWLEDGMENTS

The authors would like to acknowledge gratefully the support of the NSF Grant No. DMR 76-11427 and the expert assistance of two colleagues, Dr. James E. Kohl and William T. Cochran.

[1]The first NMR observations were made by J. Hatton and B. V. Rollin, Proc. R. Soc. A 199, 222 (1949). Detailed measurements and the correct interpretations were provided by Reif and Purcell (Ref. 11).

[2]A. F. Schuch, R. L. Mills, and D. A. Depatie, Phys. Rev. 165, 1032 (1968).

[3]G. Ahlers and W. H. Orttung, Phys. Rev. 133, A1642 (1964).

[4]K. Tomita, Proc. Phys. A 68, 214 (1955); T. Nakamura, Prog. Theor. Phys. 14, 135 (1955).

[5]N. S. Sullivan, J. Phys. (Paris) Lett. 37, L-209 (1976); N. S. Sullivan, H. Vinegar, and R. V. Pound, Phys. Rev. B 12, 2596 (1975).

[6]H. Ishimoto, K. Nagamine, and Y. Kimura, J. Phys. Soc. Jpn. 35, 300 (1973).

[7]J. H. Constable, Y. C. Shi, and J. R. Gaines, Solid State Commun. B 1, 689 (1976).

[8]P. W. Anderson, J. Phys. Soc. Jpn. 9, 316 (1954).

[9]A. Abragam, *The Principles of Nuclear Magnetism* (Oxford U. P., Oxford, 1961), Chap. 10, p. 448ff.

[10]Strictly speaking, this result is only applicable for $T = \infty$. Boltzmann population factors are introduced through the components $S_\alpha(0)$ giving

$$S(t) = e^{\lambda_u t} \sum_{i,j} p_i u_i u_j + e^{\lambda_v t} \sum_{i,j} p_i v_i v_j + e^{\lambda_w t} \sum_{i,j} p_i w_i w_j ,$$

where p_i is the relative occupation probability of state i.

[11]F. Reif and E. M. Purcell, Phys. Rev. 91, 631 (1953).

[12]J. H. Constable and J. R. Gaines, Solid State Commun. 9, 155 (1971).

[13]Y. C. Shi, J. R. Gaines, and A. Mukherjee, Phys. Lett. A 63, 342 (1977).

[14]A. Mukherjee, Y. C. Shi, and J. R. Gaines, Solid State Commun. 26, 65 (1978).
[15]J. E. Kohl, Ph.D. thesis (The Ohio State University, 1976) (unpublished).
[16]A. Mukherjee, Ph.D. thesis (The Ohio State University, 1976) (unpublished).
[17]C. C. Sung, Phys. Rev. 167, 271 (1968), Fig. 1 (W. N. Hardy and J. R. Gaines).